Available online at www.sciencedirect.com
ScienceDirect
Journal of Sound and Vibration 317 (2008) 883–897
JOURNAL OF SOUND AND VIBRATION
www.elsevier.com/locate/jsvi

Nonlinear dynamic behavior of simply supported laminated composite plates subjected to blast load

Zafer Kazancı[a,*], Zahit Mecitoğlu[b]

[a] *Aeronautical Engineering Department, Turkish Air Force Academy, 34149 Yeşilyurt, İstanbul, Turkey*
[b] *Faculty of Aeronautics and Astronautics, İstanbul Technical University, 34469 Maslak, İstanbul, Turkey*

Received 24 March 2007; received in revised form 17 March 2008; accepted 19 March 2008
Handling Editor: A.V. Metrikine
Available online 13 May 2008

Abstract

This paper deals with the analysis and discussion of nonlinear dynamic response of a laminated composite plate subjected to blast load. Dynamic equations of the plate are derived by the use of the virtual work principle. The geometric nonlinearity effects are taken into account with the von Kármán large deflection theory of thin plates. Approximate solutions for a simply supported plate are assumed for the space domain. The single term approximation functions are selected by considering the nonlinear static deformations of plate, which is obtained using finite element method. The Galerkin Method is used to obtain the nonlinear differential equations in the time domain. The finite difference method is applied to solve the system of coupled nonlinear equations. The results of approximate-numerical analysis are obtained and compared with the literature and finite element results. Good agreement is found for the character and frequencies of vibrations.

1. Introduction

Composite materials are extensively used in various engineering applications such as space stations, aircrafts, automobiles and submarines. Thin laminated composite plates are structural components, which have considerable importance to build the lightweight vehicles. The thin plates easily undergo the large amplitude vibrations if exposed to time-dependent pulses, such as blast loads occurring from fuel, bomb and nuclear explosions, gusts and sonic boom pulses.

Several studies related to the effects of air blast loading on the panel structures are investigated in the literature. Kazancı and Mecitoğlu [1] have studied the nonlinear damped vibrations of a laminated composite plate subjected to blast load. Kazancı et al. [2] have considered in-plane stiffness and inertias in the analytical solution of the laminated composite plate under blast load. Tanrıöver and Şenocak [3] have performed analytical-numerical approach on the large deflection analysis of unsymmetrically laminated composite plates.

Librescu et al. [4] have addressed the problem of the dynamic response of sandwich panels exposed to blast loadings. Nayak et al. [5–8] have investigated the transient response of composite sandwich plates by using

*Corresponding author. Tel.: +90 212 6632490x4477.
E-mail address: z.kazanci@hho.edu.tr (Z. Kazancı).

0022-460X/$ - see front matter
doi:10.1016/j.jsv.2008.03.033

new finite element formulations. Some of the parametric effects on the transient response of sandwich plates are investigated in these studies. Türkmen and Mecitoğlu [9,10] have performed some experimental, analytical and numerical studies on the nonlinear structural response of laminated composites subjected to blast load. Librescu and Nosier [11] have investigated the response of laminated composite flat panels to sonic boom and explosive blast loadings. Wei and Dharani [12] have developed a solution based on the large deflection plate theory for a laminated glass panel subjected to blast loading. Wei et al. [13] have studied the dynamic response of a laminated glass subjected to blast loading from a bomb explosion on the ground.

There have been a few studies dealing with the response of simply supported plates subjected to blast load. The analysis of simply supported orthotropic plates subject to static and dynamic loads was presented by Dobyns [14] who analyzed the response to pulses of different shapes. Louca and Pan [15] have analyzed the response of stiffened and unstiffened plates subjected to blast loading by using a single energy-based formulation. Amabili [16,17] compared theoretical and experimental results for geometrically nonlinear vibrations of rectangular plates with different boundary conditions. Chandrasekharappa and Srirangarajan [18] investigated the nonlinear response of elastic plates subjected to blast load for several boundary conditions.

However, only a few studies in the nonlinear response of simply supported laminated composite plates subjected to blast loading are investigated. Birman and Bert [19] considered the response of simply supported anti-symmetrically laminated angle-ply plates to explosive blast loading. Chen et al. [20] developed a semi-analytical finite strip method for the analysis of the nonlinear response to dynamic loading of simply supported rectangular laminated composite plates. Kazancı and Mecitoğlu [21] compared results for nonlinear dynamic behavior of a laminated composite plate subjected to blast load for different boundary conditions.

Present work includes the analyses of a simply supported laminated composite plate under blast load taking into account the in-plane stiffness and inertia effects. The geometric nonlinearity effects are taken into account with the von Kármán large deflection theory of thin plates. The equations of motion for the plate are derived by the use of the virtual work principle. Approximate displacement functions are assumed for the space domain by considering the nonlinear static deformations obtained using ANSYS software. They are substituted into the equations of motion and then the Galerkin Method is used to obtain the nonlinear differential equations in the time domain. The finite difference method is applied to solve the system of coupled nonlinear equations. The results of approximate-numerical analyses are obtained and compared with ANSYS software and literature results. Good agreement is found for the character and frequencies of vibrations.

2. Equations of motion

In this section, a mathematical model for the laminated composite plate subjected to blast load is presented. The rectangular plate with the length a, the width b, and the thickness h, is depicted in Fig. 1. The Cartesian axes are used in the derivation.

For the sake of completeness, kinematical relations can be given concisely. The strain–displacement relations for the von Kármán plate can be written as [22]

$$\varepsilon_x = \varepsilon_x^0 + z\kappa_x \tag{1a}$$

$$\varepsilon_y = \varepsilon_y^0 + z\kappa_y \tag{1b}$$

$$\varepsilon_{xy} = \varepsilon_{xy}^0 + z\kappa_{xy} \tag{1c}$$

where

$$\varepsilon_x^0 = \frac{\partial u^0}{\partial x} + \frac{1}{2}\left(\frac{\partial w^0}{\partial x}\right)^2 \tag{2a}$$

$$\varepsilon_y^0 = \frac{\partial v^0}{\partial y} + \frac{1}{2}\left(\frac{\partial w^0}{\partial y}\right)^2 \tag{2b}$$

$$\varepsilon_{xy}^0 = \frac{\partial u^0}{\partial y} + \frac{\partial v^0}{\partial x} + \frac{\partial w^0}{\partial x}\frac{\partial w^0}{\partial y} \tag{2c}$$

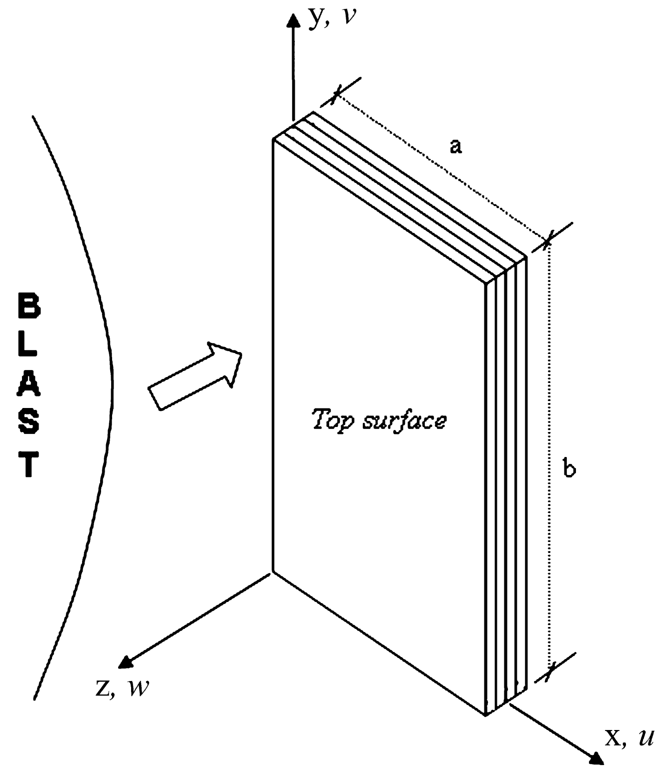

Fig. 1. Laminated composite plate.

and

$$\kappa_x = -\frac{\partial^2 w^0}{\partial x^2} \tag{3a}$$

$$\kappa_y = -\frac{\partial^2 w^0}{\partial y^2} \tag{3b}$$

$$\kappa_{xy} = -2\frac{\partial^2 w^0}{\partial x \partial y} \tag{3c}$$

where u, v and w are the displacement components in the x, y and z directions and z is the distance of the arbitrary point of the plate from the reference surface. $(\ )^0$ indicates the displacement components of reference surface. The effective elastic constants are used for defining the constitutive model of the laminated composite. The constitutive equations can then be expressed as

$$\begin{Bmatrix} \sigma_x \\ \sigma_y \\ \sigma_{xy} \end{Bmatrix} = \begin{bmatrix} \bar{Q}_{11} & \bar{Q}_{12} & \bar{Q}_{16} \\ \bar{Q}_{12} & \bar{Q}_{22} & \bar{Q}_{26} \\ \bar{Q}_{16} & \bar{Q}_{26} & \bar{Q}_{66} \end{bmatrix} \begin{Bmatrix} \varepsilon_x \\ \varepsilon_y \\ \varepsilon_{xy} \end{Bmatrix} \tag{4}$$

where σ_x, σ_y and σ_{xy} are stress components, $\bar{Q}_{ij}$'s are the elastic constants for a laminated composite. The relations between the force and moment resultants and strain components can be derived from the constitutive relations of laminated composite plate as

$$\begin{Bmatrix} \mathbf{N} \\ \mathbf{M} \end{Bmatrix} = \begin{bmatrix} \mathbf{A} & \mathbf{B} \\ \mathbf{B} & \mathbf{D} \end{bmatrix} \begin{Bmatrix} \varepsilon^0 \\ \boldsymbol{\kappa} \end{Bmatrix} \tag{5}$$

where **A**, **B** and **D** are the extensional, coupling and bending stiffness matrices, respectively. The coefficients in the matrices are

$$A_{ij} = \sum_{k=1}^{n} (\bar{Q}_{ij})_k (h_k - h_{k-1}) \tag{6}$$

$$B_{ij} = \frac{1}{2} \sum_{k=1}^{n} (\bar{Q}_{ij})_k (h_k^2 - h_{k-1}^2) \tag{7}$$

$$D_{ij} = \frac{1}{3} \sum_{k=1}^{n} (\bar{Q}_{ij})_k (h_k^3 - h_{k-1}^3) \tag{8}$$

If the blast source is distant enough from the plate, the blast pressure can be described in terms of the Friedlander exponential decay equation [23] as

$$P(t) = p_m(1 - t/t_p)e^{-\alpha t/t_p} \tag{9}$$

where the negative phase of the blast is included. In this equation, p_m is the peak blast pressure, t_p is positive phase duration, and α is waveform parameter.

Using the constitutive equations and the strain–displacement relations in the virtual work and applying the variational principles, nonlinear dynamic equations of a laminated composite plate can be obtained in terms of mid-plane displacements as follows:

$$L_{11}u^0 + L_{12}v^0 + L_{13}w^0 + N_1(w^0) + \bar{m}\ddot{u}^0 - q_x = 0 \tag{10a}$$

$$L_{21}u^0 + L_{22}v^0 + L_{23}w^0 + N_2(w^0) + \bar{m}\ddot{v}^0 - q_y = 0 \tag{10b}$$

$$L_{31}u^0 + L_{32}v^0 + L_{33}w^0 + N_3(u^0, v^0, w^0) + \bar{m}\ddot{w}^0 - q_z = 0 \tag{10c}$$

where L_{ij} and N_i denote linear and nonlinear operators, respectively. $\bar{m}$ is the mass of unit area of the mid-plane. q_x, q_y and q_z are the load vectors in the axes directions. The explicit expressions of the operators can be found in Kazancı and Mecitoğlu [1].

The boundary conditions are in the following form for a simply supported plate:

$$u^0 = v^0 = w^0 = 0 \text{ at } x = 0, a \text{ and } y = 0, b$$

$$M_x = 0 \text{ at } x = 0, a$$

$$M_y = 0 \text{ at } y = 0, b$$

and initial conditions are given by

$$u^0 = v^0 = w^0 = 0, \dot{u}^0 = \dot{v}^0 = \dot{w}^0 = 0 \text{ at } t = 0.$$

3. Methods of solution

Two methods of solution are applied to the simply supported laminated composite plate under the blast pressure: finite element solution and approximate-numerical solution.

3.1. Finite element solution

The laminated composite plate is analyzed using ANSYS finite element software. The plate is discretized using by the eight-node laminated shell elements (SHELL 91), which have geometric nonlinear capability. Four hundred elements are used for the discretization. Large deformation static analyses and transient response analyses are performed for the laminated composite plate under the blast. Transient response analysis is based on the Newmark method.

3.2. Approximate-numerical solution

The equations of motion given by Eq. (10) can be reduced in time domain by choosing some approximation functions for displacement field and applying the Galerkin method. The coupled nonlinear equations in the time domain are solved by using the finite difference method.

The approximation functions are selected so as to satisfy the natural boundary conditions

$$u^0 = \sum_{i=1}^{I}\sum_{j=1}^{J} U_{ij}(t)\phi_{ij}(x,y) \tag{11a}$$

$$v^0 = \sum_{k=1}^{K}\sum_{l=1}^{L} V_{kl}(t)\psi_{kl}(x,y) \tag{11b}$$

$$w^0 = \sum_{m=1}^{M}\sum_{n=1}^{N} W_{mn}(t)\chi_{mn}(x,y) \tag{11c}$$

The simplest multiterm approximations even results in hundreds of integral terms during the application of the Galerkin procedure and therefore they are impractical. For this reason, one-term approximation functions for the displacement components are used in this study. As mentioned by Strang [24], choosing the approximation functions is a crucial point. It should be most important for the one-term solutions.

The approximation function should closely resemble the first mode of the plate. It can be determined by considering the results of static large deformation analysis of laminated composite plate under the uniform pressure load by using ANSYS 10.0 [25] software. The approximation functions are determined by examining the finite element results obtained from the static large deformation results as follows:

$$u^0 = U_{11}(t)\sin\frac{2\pi x}{a}y^2(y-b)^2 \tag{12a}$$

$$v^0 = V_{11}(t)x^2(x-a)^2\sin\frac{2\pi y}{b} \tag{12b}$$

$$w^0 = W_{11}(t)\sin\frac{\pi x}{a}\sin\frac{\pi y}{b} \tag{12c}$$

Substituting Eq. (12) into Eq. (10) and then applying the Galerkin method [1], the time-dependent nonlinear differential equations can be obtained:

$$a_0\ddot{U} + a_1U + a_2V + a_3W + a_4W^2 + a_5 = 0 \tag{13a}$$

$$b_0\ddot{V} + b_1V + b_2U + b_3W + b_4W^2 + b_5 = 0 \tag{13b}$$

$$c_0\ddot{W} + c_1W + c_2W^2 + c_3W^3 + c_4U + c_5V + c_6UW + c_7VW + c_8 = 0 \tag{13c}$$

where the dot denotes the derivative with respect to time. The coefficients in Eq. (13) are given in the Appendix. The initial conditions can be expressed as

$$U(0) = 0, \quad V(0) = 0, \quad W(0) = 0$$

$$\dot{U}(0) = 0, \quad \dot{V}(0) = 0, \quad \dot{W}(0) = 0$$

Nonlinear coupled equations of motion are solved by using finite difference method. Therefore we may arrange Eq. (13) in the matrix format:

$$\mathbf{M}\ddot{\mathbf{Q}} + \mathbf{K}_L\mathbf{Q} + \mathbf{K}_{\mathrm{NL}}\mathbf{Q} + \mathbf{F} = 0 \tag{14}$$

where $\mathbf{Q} = \left\{ U \quad V \quad W \right\}^{\mathrm{T}}$ and $\ddot{\mathbf{Q}} = \left\{ \ddot{U} \quad \ddot{V} \quad \ddot{W} \right\}^{\mathrm{T}}$ denote the displacement and acceleration vectors, respectively. In Eq. (14), $\mathbf{M}$, $\mathbf{K}_L$ and $\mathbf{K}_{\mathrm{NL}}$ matrices are

$$\mathbf{M} = \begin{bmatrix} a_0 & 0 & 0 \\ 0 & b_0 & 0 \\ 0 & 0 & c_0 \end{bmatrix}, \mathbf{K}_L = \begin{bmatrix} a_1 & a_2 & a_3 \\ b_2 & b_1 & b_3 \\ c_4 & c_5 & c_1 \end{bmatrix}, \mathbf{K}_{\mathrm{NL}} = \begin{bmatrix} 0 & 0 & a_4 W \\ 0 & 0 & b_4 W \\ c_6 W & c_7 W & (c_2 W + c_3 W^2) \end{bmatrix} \tag{15a}$$

and $\mathbf{F}$ vector is

$$\mathbf{F} = \left\{ a_5 \quad b_5 \quad c_8 \right\}^{\mathrm{T}} \tag{15b}$$

If we replace the $\partial^2 \mathbf{Q}/\partial t^2$ term with $\partial \dot{\mathbf{Q}}/\partial t$ in Eq. (14), we can write

$$\mathbf{M} \frac{\partial \dot{\mathbf{Q}}}{\partial t} + \mathbf{K}\mathbf{Q} + \mathbf{F} = 0 \tag{16}$$

where $\mathbf{K} = \mathbf{K}_L + \mathbf{K}_{\mathrm{NL}}$. Using the definition of derivation, Eq. (16) can be written as

$$\mathbf{M} \frac{\dot{\mathbf{Q}}^{n+1} - \dot{\mathbf{Q}}^{n}}{\Delta t} + \mathbf{K}\mathbf{Q}^{n+1} + \mathbf{F} = 0 \tag{17}$$

Substituting $\dot{\mathbf{Q}}^{n+1} = \mathbf{Q}^{n+1} - \mathbf{Q}^{n}/\Delta t$ in Eq. (17) and rearranging it, we obtain

$$\left(\frac{\mathbf{M}}{(\Delta t)^2} + \mathbf{K} \right) \mathbf{Q}^{n+1} = \frac{\mathbf{M}}{\Delta t} \dot{\mathbf{Q}}^{n} + \frac{\mathbf{M}}{(\Delta t)^2} \mathbf{Q}^{n} - \mathbf{F} \tag{18}$$

Finally, if the matrices and vector given in Eq. (15) are substituted into Eq. (18), equations of motion are reduced to

$$\begin{aligned} A_1 U^{n+1} + A_2 V^{n+1} + A_3 W^{n+1} &= A_4 \\ B_1 U^{n+1} + B_2 V^{n+1} + B_3 W^{n+1} &= B_4 \\ C_1 U^{n+1} + C_2 V^{n+1} + C_3 W^{n+1} &= C_4 \end{aligned} \tag{19}$$

The coefficients in the equations are given in the appendix. From Eq. (19) we obtain the following solutions:

$$U^{n+1} = \frac{1}{A_1}[A_4 - A_2 V^{n+1} - A_3 W^{n+1}], \quad V^{n+1} = \frac{D_3 - D_2 W^{n+1}}{D_1}, \quad W^{n+1} = \frac{E_3 - E_4}{E_5} \tag{20}$$

Nonlinear terms in $\mathbf{K}_{\mathrm{NL}}$ are linearized by iterations as explained in Kazancı and Mecitoğlu [1]. The method of linearization can be stated as follows: In the first iteration we used W^n, which is known from the previous step. After the first iteration, W^{n+1} is calculated and used in place of W^n. Iteration continues until convergence criterion is obtained.

4. Numerical results

First of all, the results from the present paper are validated with literature and ANSYS results. Librescu and Nosier's [11] plate, which is labeled "Structure I", is chosen for comparison. The structure is a three-layered cross ply (0°/90°/0°) square plate whose mid-layer is two times thicker than the external ones. Ply material properties used in the analyses are given as $E_1 = 132.4$ GPa, $E_2 = 10.8$ GPa, $G_{12} = 5.6$ GPa, $\rho = 1443\,\mathrm{kg/m^3}$ and $\nu_{12} = 0.24$. The dimensions of the plate are $a = 2.54$ m, $b = 2.54$ m and $h = 0.17$ m. The analyses are performed for the uniform blast pressure. The maximum blast pressure p_m is taken to be 3447 kPa for the plate all the edges simply supported. Other parameters of Friedlander's exponential decay function given in Eq. (9) that we choose are $\alpha = 2.0$ and $t_p = 0.1$ s. Comparison of the results for the non-dimensional deflection at the center of three-layered square plate is shown in Fig. 2. As we can see from the figure, there is a good agreement among the results obtained for the chosen structure.

After this validation study, a seven-layered fiber-glass fabric with (0°/90°) fiber orientation angle for one layer is used in the numerical analyses. Ply material properties used in the analyses are taken to be $E_1 = 24.14$ GPa, $E_2 = 24.14$ GPa, $G_{12} = 3.79$ GPa, $\rho = 1800\,\mathrm{kg/m^3}$ and $\nu_{12} = 0.11$. The dimensions of the

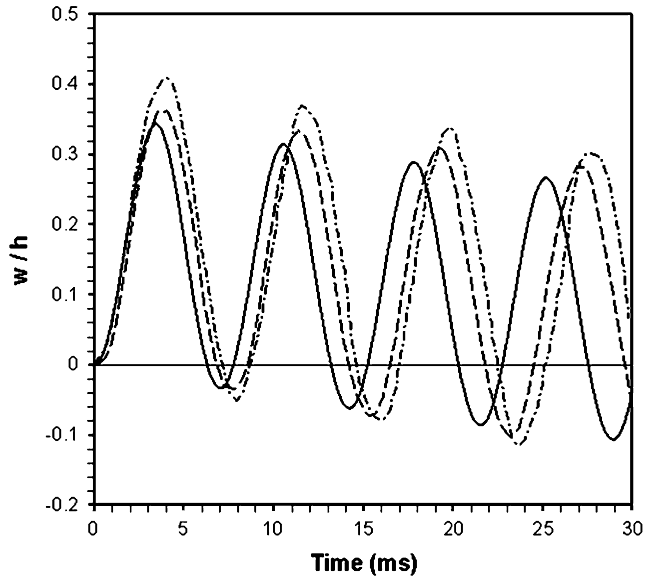

Fig. 2. Comparison of the non-dimensional deflection response of the center of a three-layered square plate: ——— approximate-numerical; - - - - - - ANSYS; . . . . Librescu and Nosier [11].

plate are $a = 0.22$ m, $b = 0.22$ m and $h = 1.96(10^{-3})$ m. The plate is assumed to be simply supported along all edges. The analyses are performed for the uniform blast pressure. The maximum blast pressure p_m is taken to be 28.9 kPa. The other parameters of the Friedlander's exponential decay function given in Eq. (9) that we choose are $\alpha = 0.35$ and $t_p = 0.0018$ s.

The solution of nonlinear coupled equations given by Eq. (13) is obtained by writing a FORTRAN program based on the finite difference scheme explained in the previous section. The convergence studies are the goal of a close proximity numerical solution. Time step convergence studies are conducted on plates subjected to 28.9 kPa peak blast load. It is found that time increment of 0.002 ms is adequate for such a numerical solution.

Fig. 3 shows the non-dimensional displacement and blast pressure variations by time. The strong suction effects considerably deflect the plate and it vibrates about this deformed shape. The maximum central deflection of the plate is three times greater than the plate thickness. The fundamental frequency of the laminated composite plate increases during the suction period due to the in-plane stiffness and geometric nonlinearities.

Figs. 4 and 5 show the variation of normal strain ε_x versus time at the bottom and top surface center of the plate, respectively. The variations of normal strain are quite different for the bottom and top surface centers in the suction period. The reasons for differences can be explained as follows: the normal strain ε_x is a combination of bending, in-plane, and nonlinear strain terms. It is well known that the values of bending term are equal at the bottom and top surfaces. If we consider the average deflected shape of the plate in the suction period as shown in Fig. 3, the sign of strain is positive at the top surface and negative at the bottom surface. The nonlinear term is always zero and the contribution of in-plane strain is always positive at the plate center. Therefore the total strain will get a large positive value at the top surface center and a small positive or negative value at the bottom surface center in the suction period. Furthermore, if the plate moves from the average deflected position in the suction direction, the plate deflection will increase and all the three terms of strain will become larger and vice versa. The contribution of the in-plane strain can be greater than that of bending strain after a certain level of plate deflection.

As can be seen from the approximate-numerical results in Figs. 4 and 5, there is a minimum bounding strain value in the strain–time histories due to the nonlinear action of the laminated composite plate and the normal strain on the top surface center is more critical than that of the bottom surface center with respect to failure.

Time histories of normal strain in the x direction at different points of the plate's top surface are shown in Fig. 6. The maximum normal strain occurs at the center of the plate. The normal strain ε_x at the plate edge

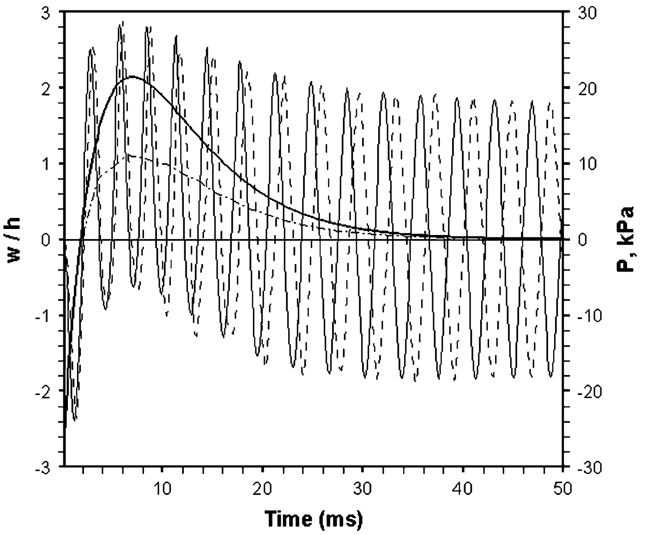

Fig. 3. Time history of dimensionless central deflection: - - - - - - ANSYS; ——— approximate-numerical; . . . . approximate-numerical(average); ━━━━ blast load.

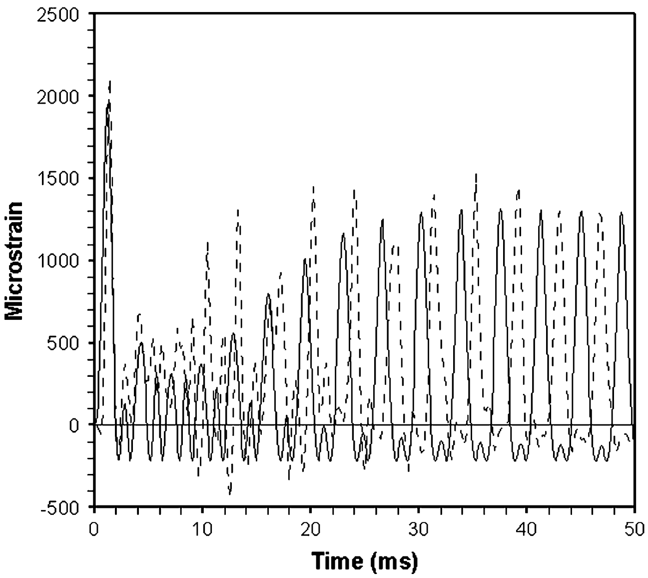

Fig. 4. Comparison of the strain–time history results at the center of bottom surface: - - - - - - ANSYS; ——— approximate-numerical.

($x = 0$) is always positive but the strains at the quarter and half-span can take small negative values during the oscillation. The time history character of the strain at the plate edge shows a considerable difference from the others during the free vibration phase of oscillation.

Fig. 7 shows that the time histories of dimensionless central deflections at the center of plates which have different aspect ratios. The results are obtained for the aspect ratios of 1.00, 0.75, 0.50 and 0.25 by keeping the plate area constant. A comparison of strain (ε_x) time history results for the plates, which have different aspect ratios is also shown in Figs. 8 and 9 for the center of bottom and top surfaces, respectively. The analyses are performed for the seven-layered fiber-glass fabric that has [0°/90°] fiber orientation. The deflection amplitude increases and the frequency of vibration decreases while the aspect ratio of plate increases, seen in Fig. 7. On the other hand, while the aspect ratio of the plate decreases, the minimum bounding value of ε_x increases for

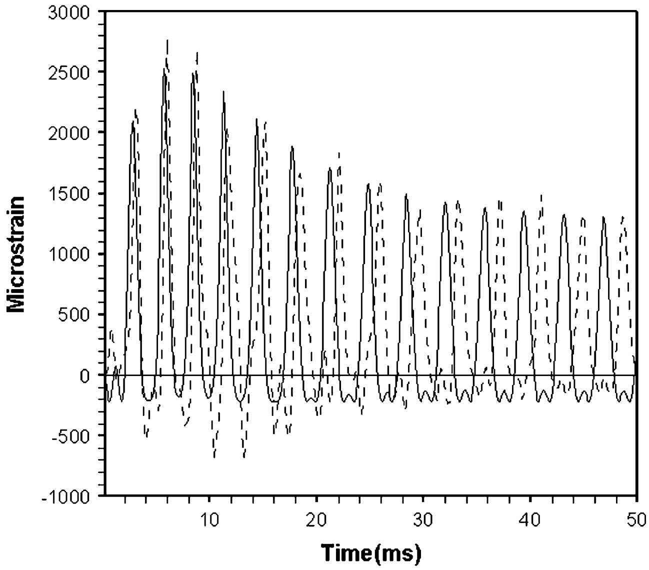

Fig. 5. Comparison of the strain-time history results at the center of top surface: ------ ANSYS; ——— approximate numerical.

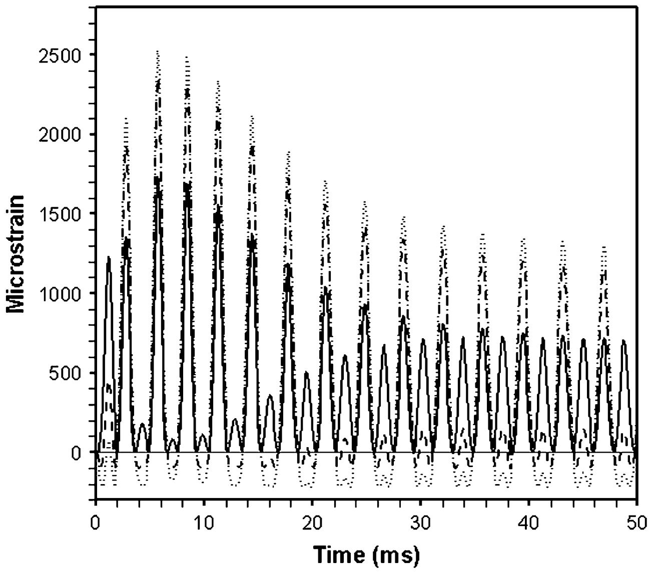

Fig. 6. Time histories of normal strain ε_x at the different points of the plate's bottom surface: ——— $x = 0$; ------ $x = a/4$; ········· $x = a/2$.

the bottom surface center, as shown in Fig. 8. Although the peak value of strain increases with decrease in aspect ratio for the bottom surface center, the peak value of the strain at the top center takes a maximum value for the aspect ratio 0.5. The frequency of the strain oscillation increases with the decrease in aspect ratio as expected. Minimum peak strains for the both surfaces occur for the aspect ratio 1, i.e. square plate.

For the different layer numbers, the time histories of dimensionless central deflections at the center of plate are shown in Fig. 10. The displacement amplitudes of plates decrease while the plate layer number, and so the plate thickness, increases. Higher plate deflections due to the suction are observed for the thin plates as expected. If only the plate bending stiffness is considered, it is anticipated that the amplitude of vibration

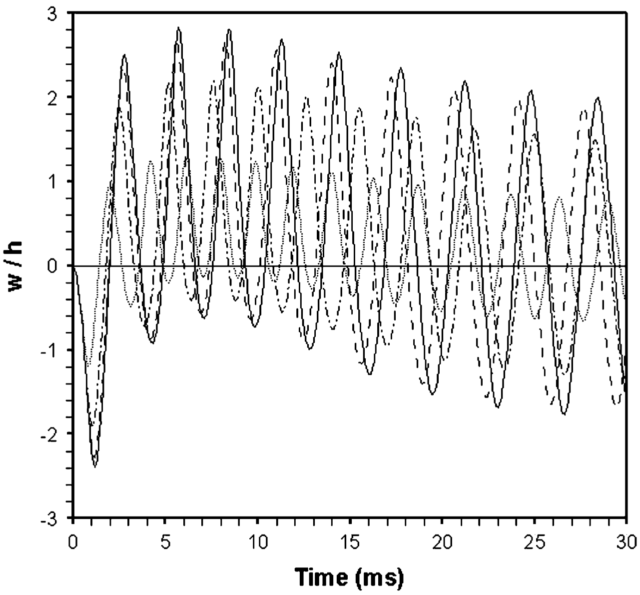

Fig. 7. Effect of aspect ratio on deflection time history: —— $a/b = 1.00$; - - - - - $a/b = 0.75$; - . - . - . $a/b = 0.50$; ·········· $a/b = 0.25$.

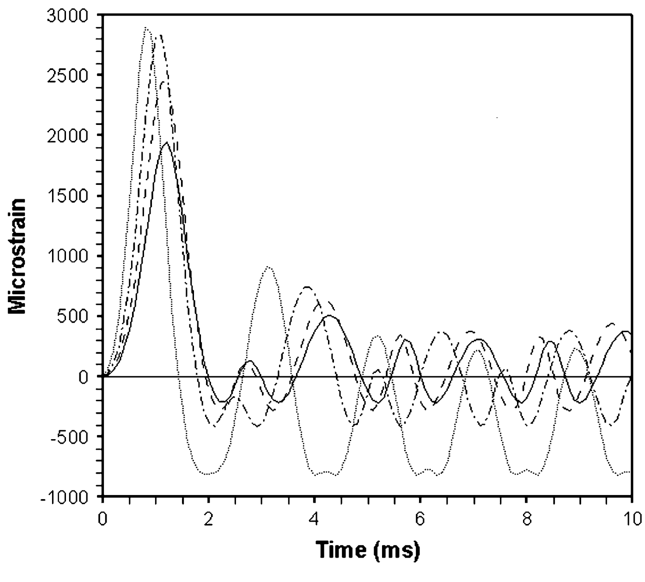

Fig. 8. Comparison of the strain–time histories for different aspect ratios at the center of bottom surface: —— $a/b = 1.00$; - - - - - $a/b = 0.75$; - . - . - . $a/b = 0.50$; ·········· $a/b = 0.25$.

should exhibit a much greater increase with the decreasing layer number. However, increase in the in-plane stiffness and nonlinear actions with the increasing plate deflection plays a role in reducing the plate deflection. The vibration frequency of the plates increases with the layer number. The strain-time history results at the centers of bottom and top surfaces are shown in Figs. 11 and 12, respectively. As seen from Fig. 11, the absolute value of minimum bounding strain raises with the increasing layer number. On the other hand the peak value of the strain decrease with the increasing layer number as shown in Figs. 11 and 12. These results can be explained as follows: The relative effects of geometric nonlinearity decrease with the layer

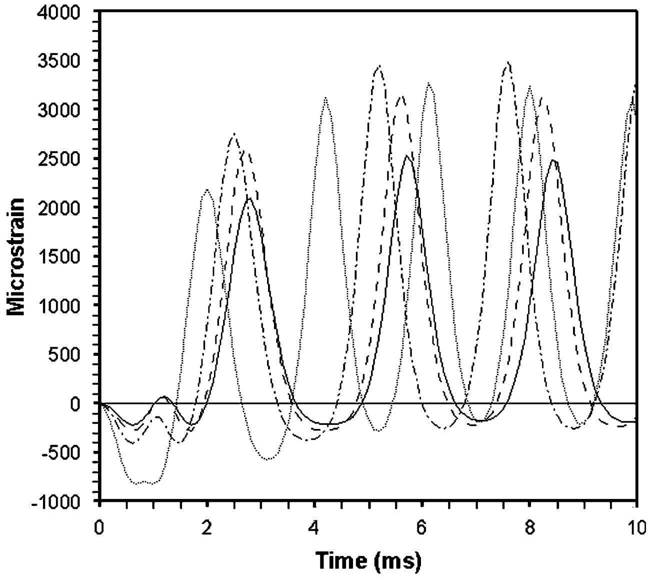

Fig. 9. Comparison of the strain–time histories for different aspect ratios at the center of top surface: ——— $a/b = 1.00$; - - - - - - $a/b = 0.75$; - · - · - · - · - $a/b = 0.50$; ············ $a/b = 0.25$.

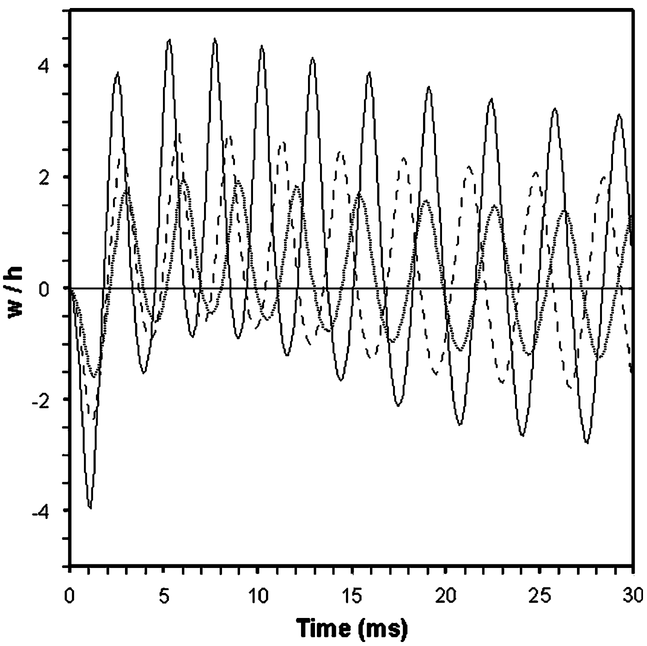

Fig. 10. Effect of layer number on deflection time history: ——— 5; - - - - - - 7; ············ 9.

number, since the ratio of maximum deflection to the plate thickness decreases with the increasing layer number. As a result, the relative contribution of the bending strain term increases in comparison to the in-plane and nonlinear strain terms. Therefore, while the layer number increases the minimum bounding value of strain increases and the expected decrease in strain does not occur as observed in the linear behavior.

Different fiber orientations for the simply supported plate are considered in this study but any significant effect of the fiber orientation on the dynamic behavior is not found.

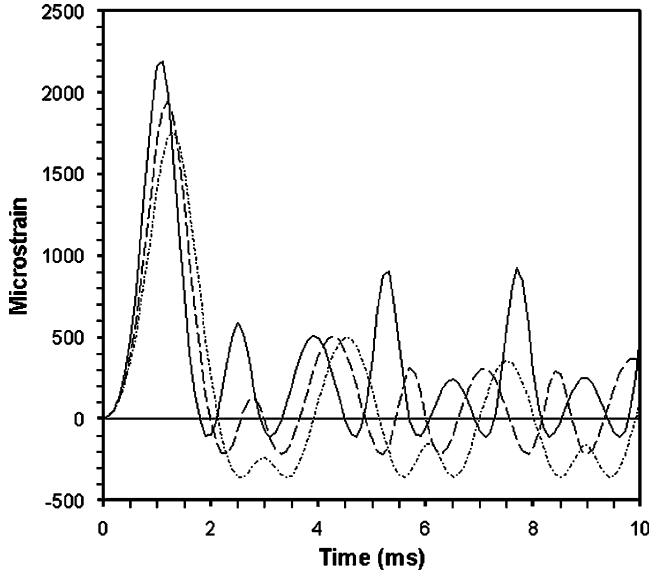

Fig. 11. Effect of layer number on the strain–time history at the center of bottom surface: ——— 5; - - - - - - 7; ············ 9.

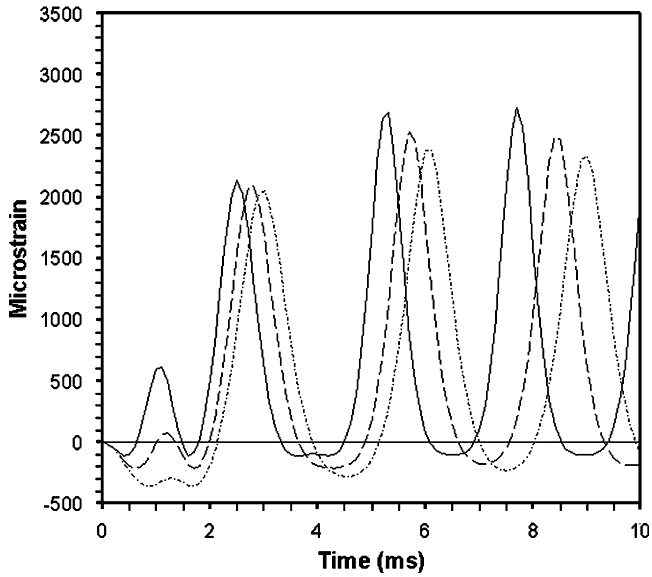

Fig. 12. Effect of layer number on the strain–time history at the center of top surface: ——— 5; - - - - - - 7; ············ 9.

5. Conclusions

In this study, the equations of motion of the laminated composite rectangular plates under blast load are derived in the frame of the von Kármán large deflection theory of thin plates. The Galerkin method is used to obtain a set of the nonlinear differential equations in the time domain. The finite difference method is applied to solve the system of coupled nonlinear equations. The approximate-numerical results are compared with the literature and ANSYS finite element results. Good agreement is found for the character and frequencies of vibrations.

A parametric study is conducted, considering the effects of aspect ratio, fiber orientation and layer number. While the aspect ratio of the plate increases, the amplitude of the normal strain variation decreases, and the corresponding frequency increases. The fiber orientations have negligible effect on the vibration characteristics, since the plates are laminated from the fabric with (0°/90°) fiber orientation angle for one layer.

The aspect ratio decrease results in a decrease of vibration amplitude and an increase of vibration frequency. The layer number increase causes lower amplitudes of vibration as expected. However, vibration frequency decreases while the layer number increases, unexpectedly. If the larger deflections as a result of thinner plate are considered, it can be deduced that the nonlinear and in-plane stiffness effects will increase in the case of thinner plate and it can result in a higher vibration frequency than that of the thicker plate. The peak values of the strain decrease with increasing layer number.

Other boundary conditions can be analyzed using the same method. The effect of the blast pressure character on the dynamic behavior can be investigated. The sandwich plates with laminated face sheets can be analyzed by using the same method. Future studies may be devoted on these subjects.

Acknowledgments

The authors wish to thank T.R. Prime Ministry State Planning Organization for its support of Project No. 901341998k121980 entitled 'Investigation of explosion effects on structures'.

Appendix

Coefficients in the time-dependent nonlinear differential equations:

$$a_0 = \frac{ab^9}{1260}\bar{m}, \quad a_1 = \frac{3a^2A_{66}b^7 + A_{11}b^9\pi^2}{315a}$$

$$a_2 = \frac{9a^4b^4(A_{12}+A_{66})}{\pi^6}, \quad a_3 = \frac{16b^3(b^2B_{11} + a^2(B_{12}+2B_{66}))(-12+\pi^2)}{3a^2\pi^3}$$

$$a_4 = \frac{b^3(A_{11}b^2(45+\pi^4) + a^2(90A_{66} - A_{12}(-45+\pi^4))}{240a^2\pi}$$

$$a_5 = 0$$

$$b_0 = \frac{9a^9b}{1260}\bar{m}, \quad b_1 = \frac{3a^7b^2A_{66} + a^9A_{22}\pi^2}{315b}$$

$$b_2 = \frac{9a^4b^4(A_{12}+A_{66})}{\pi^6}, \quad b_3 = \frac{16a^3(a^2B_{22} + b^2(B_{12}+2B_{66}))(-12+\pi^2)}{3b^2\pi^3}$$

$$b_4 = \frac{a^3(A_{22}a^2(45+\pi^4) + b^2(90A_{66} - A_{12}(-45+\pi^4)))}{240b^2\pi}$$

$$b_5 = 0$$

$$c_0 = \frac{ab}{4}\bar{m}, \quad c_1 = \frac{(b^4D_{11} + a^4D_{22} + 2a^2b^2(D_{12}+2D_{66}))\pi^4}{4a^3b^3}$$

$$c_2 = \frac{8(B_{12}-B_{66})\pi^2}{3ab}, \quad c_3 = \frac{(9a^4A_{22} + 2a^2(3A_{12}+4A_{66})b^2 + 9A_{11}b^4)\pi^4}{128a^3b^3}$$

$$c_4 = \frac{(16b^3(4b^2B_{11} + a^2(B_{12}+2B_{66})))(-12+\pi^2)}{3a^2\pi^3}, \quad c_5 = \frac{(16a^3(4a^2B_{22} + b^2(B_{12}+2B_{66})))(-12+\pi^2)}{3b^2\pi^3}$$

$$c_6 = \frac{3b^3(A_{12}+A_{66})}{4\pi} + \frac{A_{11}((b^5/60)+(3b^5/4\pi^4))\pi^3}{2a^2} - \frac{A_{12}(b^5/60+3b^5/4\pi^4)\pi^3}{2b^2}$$

$$c_7 = \frac{3a^3(A_{12}+A_{66})}{4\pi} + \frac{A_{22}((a^5/60)+(3a^5/4\pi^4))\pi^3}{2b^2} - \frac{A_{12}((a^5/60)+(3a^5/4\pi^4))\pi^3}{2a^2}$$

$$c_8 = -\frac{4ab}{\pi^2} q_z$$

Coefficients in the finite difference equations:

$$A_1 = \frac{a_0}{(\Delta t)^2} + a_1, \quad A_2 = a_2, \quad A_3 = a_3 + a_4 W^n, \quad A_4 = \frac{a_0}{\Delta t}\dot{U}^n + \frac{a_0}{(\Delta t)^2} U^n - a_5,$$

$$B_1 = b_2, \quad B_2 = \frac{b_0}{(\Delta t)^2} + b_1, \quad B_3 = b_3 + b_4 W^n, \quad B_4 = \frac{b_0}{\Delta t}\dot{V}^n + \frac{b_0}{(\Delta t)^2} V^n - b_5,$$

$$C_1 = c_4 + c_6 W^n, \quad C_2 = c_5 + c_7 W^n, \quad C_3 = \frac{c_0}{(\Delta t)^2} + c_1 + c_2 W^n + c_3 (W^n)^2,$$

$$C_4 = \frac{c_0}{\Delta t}\dot{W}^n + \frac{c_0}{(\Delta t)^2} W^n + c_8$$

$$D_1 = B_2 - \frac{B_1 A_2}{A_1}, \quad D_2 = B_3 - \frac{B_1 A_3}{A_1}, \quad D_3 = B_4 - \frac{B_1 A_4}{A_1},$$

$$E_1 = C_2 - \frac{C_1 A_2}{A_1}, \quad E_2 = C_3 - \frac{C_1 A_3}{A_1}, \quad E_3 = C_4 - \frac{C_1 A_4}{A_1}, \quad E_4 = \frac{E_1 D_3}{D_1}, \quad E_5 = E_2 - \frac{E_1 D_2}{D_1}.$$

References

[1] Z. Kazancı, Z. Mecitoğlu, Nonlinear damped vibrations of a laminated composite plate subjected to blast load, *AIAA Journal* 44 (9) (2006) 2002–2008.

[2] Z. Kazancı, Z. Mecitoğlu, A. Hacıoğlu, Effect of in-plane stiffnesses and inertias on dynamic behavior of a laminated composite plate under blast load, *Proceedings of Ninth Biennial ASCE Aerospace Division International Conference on Engineering, Construction, and Operations in Challenging Environments, Earth & Space-2004*, 2004, pp. 484–491 7–10 March.

[3] H. Tanrıöver, E. Şenocak, Large deflection analysis of unsymmetrically laminated composite plates: analytical-numerical type approach, *International Journal of Non-Linear Mechanics* 39 (2004) 1385–1392.

[4] L. Librescu, S.Y. Oh, J. Hohe, Linear and non-linear dynamic response of sandwich panels to blast loading, *Composites: Part B* 35 (2004) 673–683.

[5] A.K. Nayak, R.A. Shenoi, S.S.J. Moy, Transient response of composite sandwich plates, *Composite Structures* 64 (2004) 249–267.

[6] A.K. Nayak, R.A. Shenoi, S.S.J. Moy, Transient response of initially stressed composite sandwich plates, *Finite Elements in Analysis and Design* 42 (10) (2006) 821–836.

[7] A.K. Nayak, S.S.J. Moy, R.A. Shenoi, Quadrilateral finite elements for multilayer sandwich plates, *Journal of Strain Analysis for Engineering Design* 38 (5) (2003) 377–394.

[8] A.K. Nayak, R.A. Shenoi, S.S.J. Moy, Dynamic response of composite sandwich plates subjected to initial stresses, *Composites Part A—Applied Science and Manufacturing* 37 (8) (2006) 1189–1205.

[9] H.S. Türkmen, Z. Mecitoğlu, Nonlinear structural response of laminated composite plates subjected to blast loading, *AIAA Journal* 37 (12) (1999) 1639–1647.

[10] H.S. Türkmen, Z. Mecitoğlu, Dynamic response of a stiffened laminated composite plate subjected to blast load, *Journal of Sound and Vibration* 221 (3) (1999) 371–389.

[11] L. Librescu, A. Nosier, Response of laminated composite flat panels to sonic boom and explosive blast loadings, *AIAA Journal* 28 (2) (1990) 345–352.

[12] J. Wei, R.L. Dharani, Response of laminated architectural glazing subjected to blast loading, *International Journal of Impact Engineering* 32 (12) (2006) 2032–2047.

[13] J. Wei, M.S. Shetty, R.L. Dharani, Stress characteristics of a laminated architectural glazing subjected to blast loading, *Computers & Structures* 84 (2006) 699–707.

[14] A.L. Dobyns, Analysis of simply-supported orthotropic plates subject to static and dynamic loads, *AIAA Journal* 19 (1981) 642–650.
[15] L.A. Louca, Y.G. Pan, Response of stiffened and unstiffened plates subjected to blast loading, *Engineering Structures* 20 (1998) 1079–1086.
[16] M. Amabili, Nonlinear vibrations of rectangular plates with different boundary conditions: theory and experiments, *Computers & Structures* 82 (2004) 2587–2605.
[17] M. Amabili, Theory and experiments for large-amplitude vibrations of rectangular plates with geometric imperfections, *Journal of Sound and Vibration* 291 (2006) 539–565.
[18] G. Chandrasekharappa, H.R. Srirangarajan, Nonlinear response of elastic plates to pulse excitations, *Computers & Structures* 27 (1987) 373–378.
[19] V. Birman, C.W. Bert, Behaviour of laminated plates subjected to conventional blast, *International Journal of Impact Engineering* 6 (1987) 145–155.
[20] J. Chen, D.J. Dawe, S. Wang, Nonlinear transient analysis of rectangular composite laminated plates, *Composite Structures* 49 (2000) 129–139.
[21] Z. Kazancı, Z. Mecitoğlu, Nonlinear dynamic behavior of a laminated composite plate subject to blast load for different boundary conditions, *Ankara International Aerospace Conference (AIAC 2005)*, Ankara, Turkey, 2005, paper AIAC 2005-044.
[22] R.F. Gibson, *Principles of Composite Material Mechanics*, McGraw-Hill, New York, 1994.
[23] A.D. Gupta, F.H. Gregory, R.L. Bitting, S. Bhattacharya, Dynamic analysis of an explosively loaded hinged rectangular plate, *Computers & Structures* 26 (1987) 339–344.
[24] G. Strang, *Introduction to Applied Mathematics*, Wellesley-Cambridge Press, Wellesley, MA, 1986.
[25] ANSYS 10.0 Commercial Software.